water

MDPI

Article

Experimental Study on the Characteristics of Sediment Transport and Sorting in Pressurized Pipes

Yan Li [1], Jinliang Zhang [1,2,*], Haijue Xu [1] and Yuchuan Bai [1]

[1] Institute for Sedimentation on River and Coastal Engineering, Tianjin University, Tianjin 300072, China; yantai_fan@163.com (Y.L.); xiaoxiaoxu_2004@163.com (H.X.); ychbai@tju.edu.cn (Y.B.)
[2] Yellow River Engineering Consulting Co., Ltd., Zhengzhou 450003, China
* Correspondence: jlzhangyrec@126.com

Abstract: Sediment transport in pipes is an effective engineering measure used to reallocate water–sediment resources and is widely used in reservoir flooding and sediment discharging, river dredging, floodplain area deposition, as well as other projects. An experimental investigation of sediment transport in pressurized pipes, with heterogeneous sediment (d_{50} = 107 μm) of the lower Yellow River as the experimental material, is presented. This study mainly explored the change law of sediment transport and sorting in pressure pipes with an internal diameter of 0.08 m. The experimental results reveal that the presence of sediment significantly changed the distribution of the flow velocity field. At the same flow rate, the velocity of the lower water body with a high sediment concentration decreased, while that of the upper water body increased. At a low water flow rate, the increase in sediment concentration caused an asymmetric distribution of the cross-sectional velocity. The vertical concentration decreased in height, and the obvious stratification of vertical sediment particles was observed. With the increase in the flow rate, the asymmetry of the velocity distribution significantly decreased, the concentration profile tended towards being uniformly distributed along the vertical direction, and the separation effect of the sediment particles weakened.

Keywords: pipe experiment; heterogeneous sediment; velocity distribution; sediment concentration profile; sediment sorting

Citation: Li, Y.; Zhang, J.; Xu, H.; Bai, Y. Experimental Study on the Characteristics of Sediment Transport and Sorting in Pressurized Pipes. *Water* **2021**, *13*, 2782. https://doi.org/10.3390/w13192782

Academic Editor: Bommanna Krishnappan

Received: 20 August 2021
Accepted: 1 October 2021
Published: 7 October 2021

1. Introduction

Sediment transport and sorting is a common phenomenon whose use is widespread in rivers, reservoirs, estuaries and coastal areas. In fact, sediment transport and sorting is also a redistribution process of water–sediment resources. Pipeline hydraulic transport has the advantages of high efficiency, good continuity and large transport volume [1–7], and is widely used in many aspects such as flood discharge and sediment discharge in reservoirs, water and sediment diversion along rivers, river dredging and sediment deposition in floodplains. It is also an important means of reallocating sediment resources.

In the process of water–sediment movement, sediment particles move forward in the form of a bed load or suspended load due to the turbulence of water flow and the nonuniformity of sediment particles. While the fluid properties change due to the increase in fine sediment particles, its flow characteristics and sediment transport characteristics, including its flow state conversion characteristics [8,9], turbulence energy dissipation characteristics [10–12], sediment sorting characteristics [13–16], sedimentation patterns [17] and sediment transport and flushing [18], all change significantly. From the perspective of solid–liquid two-phase flow, some authors have established a two-phase flow model to explore the characteristics of water–sediment movement and analyze the distribution law of the sediment concentration profile [19]. For example, Pu et al. [20] proposed a linear-power couple model combining the sediment size, Rouse number, mean concentration and flow depth parameters to model the sediment profile due to the differences between hyperconcentrated and dilute flows. Liang et al. [21] proposed a mixture model for sediment-laden flows based on Eulerian–Eulerian two-phase flow theory, and the calculation speed can be effectively improved while maintaining the calculation accuracy. Although research on two-phase flow models has greatly progressed in recent years, their application in pipeline sediment transport is not mature enough. The movement of water–sediment in pipelines is actually a complicated movement of solid–liquid two-phase flow, which is much more complicated than that in open channels.

From the perspective of engineering applications, the two most important issues in the study of pipeline transportation processes are the influence of sediment movement on energy dissipation and the sediment deposition law in the process of pipeline transportation [22]. Regarding the problem of sediment deposition inside the pipeline, some researchers have measured the evolution of sediment at the bottom of a pipeline and analyzed the physical and chemical characteristics of the sediment, as well as the characteristics of the sediment's movement [23,24]. Some researchers have conducted in-depth research on critical sediment deposition velocity [7,22,23,25], resistance loss [26,27] and other related topics. However, as a complex two-phase flow movement, pipeline sediment transport still has space for further research. In pressurized pipelines, the movement properties of heterogeneous sediment and sediment particle vertical sorting are valuable topics for further research. In addition, in an actual pipeline transport project, the sediment-laden flow contains different sediment particle sizes, and the relative position and velocity of these sediment particles play an important role in the design and operation of the pipeline. Sediment deposition directly affects the operation stability and sediment transport efficiency of the pipeline. Due to the high friction resistance loss caused by the siltation of coarse particles and the continuous erosion and corrosion of the pipe wall, the sediment transport is blocked, the operating cost increases and the sediment leakage caused by pipeline failure affects the local environment [7].

To improve the efficiency and service life of pipelines used for transportation, it is necessary to understand the physical characteristics of velocity distribution, concentration profile and sediment sorting in pipes. The present study aimed to establish a physical test model of pipe sediment transport based on the engineering background of the hyperconcentrated sediment tunnel and sediment transport pipe of the reservoir in the Yellow River Basin. The objectives of this study were to (1) explore the influence of sediment concentration variation on the velocity distribution in pressure pipes; (2) analyze the changes in the sediment concentration and transport flux in the vertical direction; and (3) discuss the effects of different sediment concentrations on vertical sediment particle separation.

2. Materials and Methods

2.1. Experimental Facility

All experiments were carried out in a closed-circuit pipe which was approximately 40.0 m long and 0.08 m in internal diameter. The pipeline is horizontally arranged approximately 0.3 m from the ground surface, and it is fixed to the ground by a bracket placed at one-meter intervals. Figure 1 illustrates the experimental setup. There is a 0.5 m connecting hose between the pipe and centrifugal pump to eliminate the pipe vibration caused by the centrifugal pump. Butterfly valves were placed near the inlet and outlet of the pipe for flow rate control and sediment concentration measurement, and an electromagnetic flowmeter was placed at least 5 m from the site of flow injection into the pipe. Valve 2 and 3 were used to control discharge, and valves 1 and 4 were used to collect sediment-laden flow from the pipe, as shown in Figure 1a.

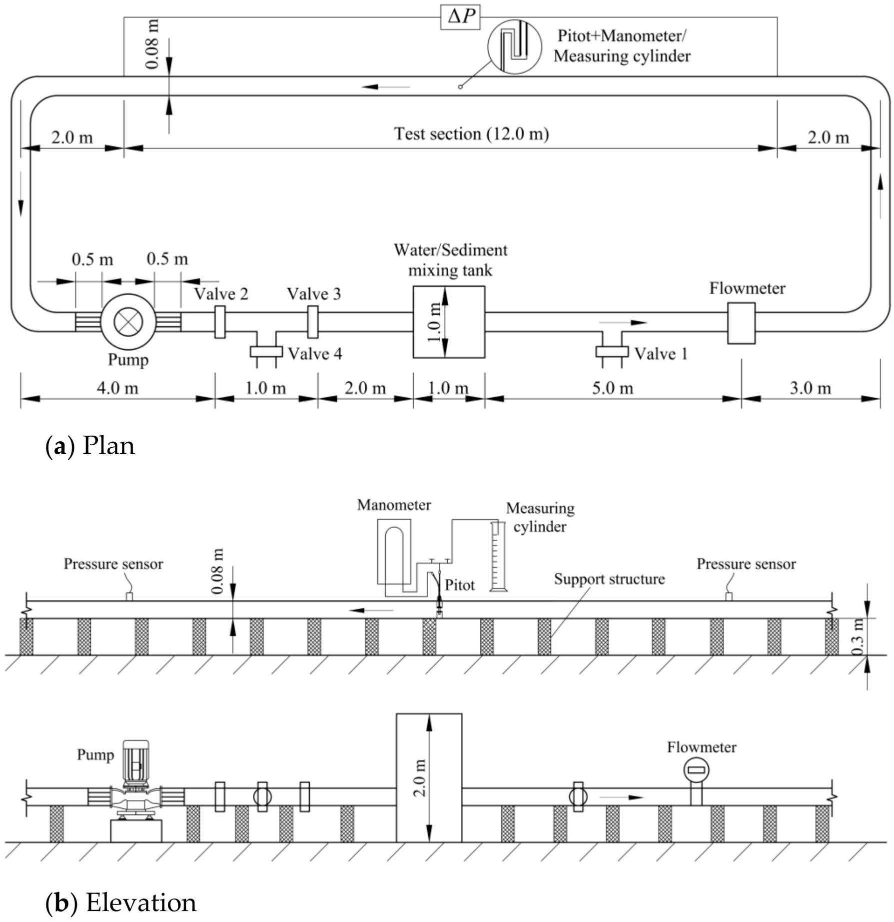

Figure 1. Sketch of the circulating pipe experimental system (not to scale).

The length of the working test section of the plexiglass pipe was 12.0 m, and the sediment movement in the pipe could be observed. A pressure sensor was installed on both sides of the test section to detect pressure changes, and a Pitot tube (including manometer) was arranged in the middle to measure the longitudinal velocity inside the pipe. The sediment sampling in this experiment was a kind of sampling method similar to siphon pipes [28]. The sediment samples in the pipe could be obtained by the existence of a pressure difference inside and outside the pipe, which is different from the isokinetic sampling (i.e., the velocity within the sampling tube has to be the same as the velocity in the pipe at the location of measurement) [29]. The measuring steps were as follows: (1) the total pressure tube outlet position connected to the measuring cylinder (Figure 1b); (2) the slurry sample was siphoned out through the total pressure tube due to the pressure difference inside and outside the pipe; (3) the volume of slurry in the measuring cylinder was recorded; (4) the sediment concentration was calculated by drying and weighing the slurry sample; and (5) the steps above were repeated, and the sediment concentrations at different positions along the vertical direction were obtained. The dried sediment samples can be used to analyze the sediment gradation curve by a particle size analyzer. Figure 2 is the sketch of an improved Pitot tube, wherein the total pressure hole (#1) is aligned in the flow direction and the static pressure hole (#2) is aligned on both sides of the Pitot tube, perpendicular to the flow direction. The hole diameter was approximately 1.5 mm, less than 1/50 of the pipe internal diameter (80.0 mm).

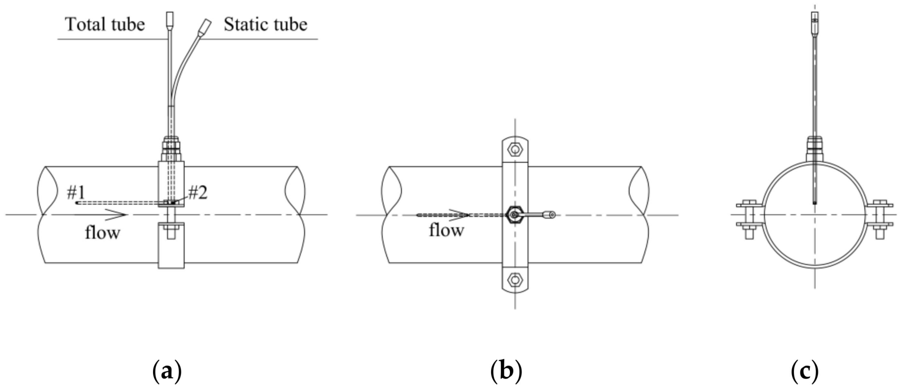

Figure 2. Improved Pitot tube schematic diagram: (**a**) longitudinal; (**b**) plan; and (**c**) section.

In this experiment, the lower Yellow River fine sediment from the floodplain area of Jiyang in Shandong Province was selected as the test material, and the sediment sample density was approximately 2650 kg/m^3. There are two main considerations for choosing sediment in the lower Yellow River: (1) the physical test model of pipe sediment transport based on the engineering background of the hyperconcentrated sediment tunnel and the sediment transport pipe of the reservoir; and (2) the sediment particle size in the lower reaches of the Yellow River is larger than that in the upper reservoir area. Natural sediment with a median particle size slightly larger than that in the upper reservoir area was selected as the experimental material, and the kinematic viscosity coefficient was less than that of the sediment in the reservoir area. An ultrafast Malvern 3000 intelligent particle size analyzer (Malvern Instruments Ltd., Malvern, UK) was used for the particle size analysis of sediment samples, and the measurement range of the instrument was 0.01–3500 µm. Compared with the sedimentation method and sieve analysis method, the laser particle size analyzer has the advantages of fast speed, good repeatability and high measurement accuracy [30]. Laser diffraction technology was used to measure the particle size. When a laser beam passes through a dispersed particle sample, the intensities of light scattered from particles of different sizes are different. The volume ratio of different sediment particles was obtained by analyzing and calculating the scattering spectrum. According to the analytical results, a sediment particle size distribution diagram was created, as shown in Figure 3. The distribution of particle sizes is narrow, and the gradient of the grading curve is steep, which indicates that the particle size of the sediment sample is relatively uniform. The d_{25}, d_{50} and d_{75} of the sediment particles are 73, 107 and 133 µm, respectively, and the degree of nonuniformity $\varphi = d_{75}/d_{25} = 1.82$.

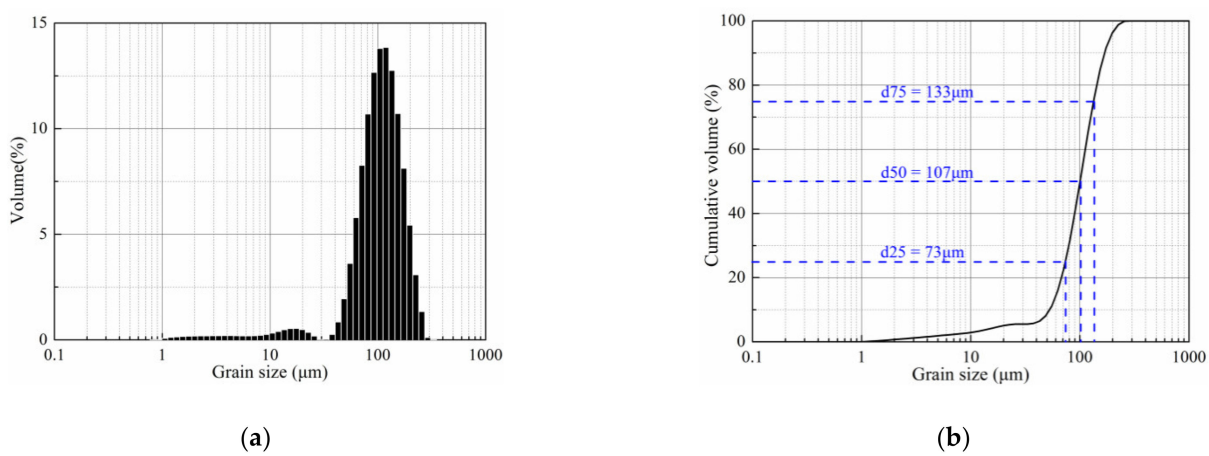

Figure 3. Sediment particle distribution: (**a**) histogram; and (**b**) cumulative size distribution.

2.2. Test Conditions

The velocity distribution and sediment concentration distribution were measured under conditions of full turbulence and relatively stable sediment concentration in the pipe. This experiment includes two working conditions, clear water and muddy water, in which clear water conditions are taken as the reference group, with a discharge range of 5.05–50.13 m^3/h. The discharge range in the pipe can be controlled by adjusting butterfly valves 2 and 3 after the pipe pump. The muddy water discharge ranges from 5.81 to 40.29 m^3/h, and the sediment volume concentration ranges from 2.2 to 26.27%, as shown in Table 1.

Table 1. Pipe/sediment properties and sediment concentration conditions.

Pipe Diameter *D*/mm	Discharge *Q*/m³/h	Range of Grain Sizes *d*/μm	Range of Volume Concentrations C/%
80	5.05–50.13	-	0
80	5.81–40.29	0.82–323	2.2–26.27

These tests were conducted in the turbulent regime with Reynolds' numbers ranging from 2.2×10^4 to 2.7×10^5. To ensure that the measured data were obtained at a relatively stable sediment concentration in the pipe, the following measures were taken: (1) the pool was equipped with a spiral agitator to continuously stir the muddy water to ensure that sediment could fully enter the circulating pipeline; (2) after the sediment flow entered the pipeline for a period of time, the sediment concentrations were measured through the valves at the inlet and outlet of the pipeline and compared. If the value was large, the group test was carried out again; (3) the Pitot tube was set up in the middle of the pipeline test section. The vertical sediment concentration of the pipeline can be obtained by the stratified sampling method and compared with the sediment concentrations measured at the inlet and outlet.

3. Results and Discussion

3.1. Velocity Distribution

Turbulence motion, whether in laboratory model experiments or natural rivers, is an important form of water movement. By analyzing the velocity distribution caused by the change in sediment concentration in the pipe, the physical mechanism of the change in velocity structure in the pressurized pipe can be investigated. When clear water is transported in the pressurized pipe, the measurement results show that the velocity of the circular pipe section has an axisymmetric distribution. Figure 4 shows the measured velocity distribution from the bottom wall to the central axis of the pipe ($0 \leq y \leq R$). The distribution of the mean flow velocity in the turbulent flow of clear water is generally described by the logarithmic flow velocity formula:

$$\frac{u_m - u}{u_*} = \frac{1}{\kappa} \ln \frac{y_m}{a} \tag{1}$$

where u_m is the maximum velocity of the flow; u_* is the shear velocity, i.e., $u_* = \sqrt{\tau_w/\rho}$, whereas τ_w is the shear stress acting on the pipe walls, i.e.,$\tau_w = \rho g R J/2$; ρ is the density of the liquid; J is the horizontal pipe slurry energy slope; u is the time-averaged velocity at a distance a from the pipe wall; k is the von Kármán constant (in clear water, K value is 0.40); and y_m is the location of the maximum velocity in the vertical direction.

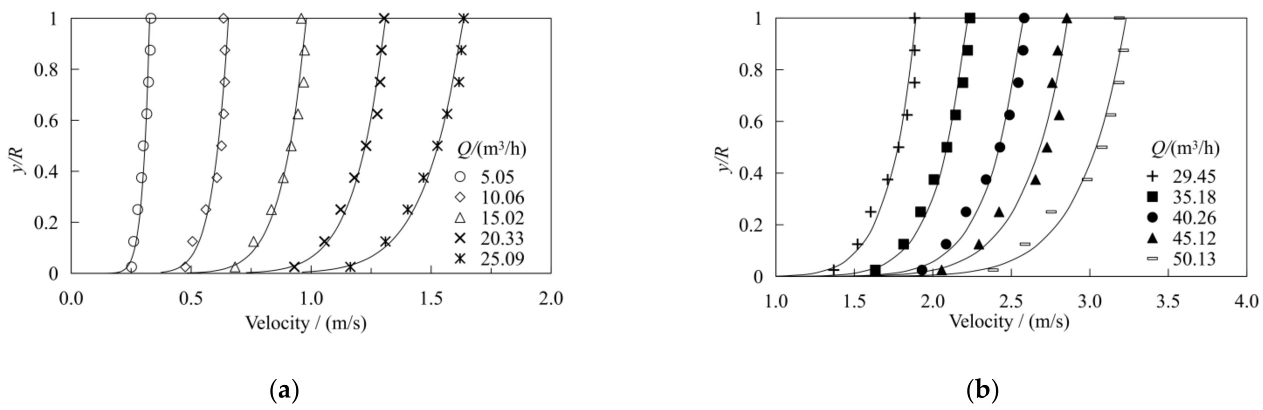

Figure 4. Observed clear water velocity distribution with different flow discharges: (**a**) Q = 5.05–25.09 m^3/h; and (**b**) Q = 29.45–50.13 m^3/h.

Figure 5 shows a velocity profile in a circular pipe under clear water conditions which agrees with a logarithmic distribution, and Table 2 lists the shear velocity under different flow rate conditions.

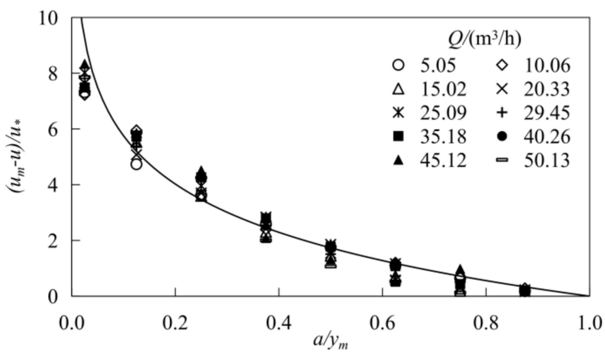

Figure 5. Theoretical curve and experimental data in the clear water pipe.

After the flow is mixed with sediment, it changes from clear water to water–sediment two-phase flow, resulting in obvious changes in the flow movement characteristics and velocity structure. Figure 6 shows a schematic diagram of the water–sediment two-phase flow in the pipe.

Table 2. Shear velocity for different flow rates under clear water conditions.

Discharge $Q/m^3/h$	Head Loss H_f/cm	Energy Slope J	Shear Stress $\tau_w/N/m^2$	Shear Velocity u_*/m/s
5.05	1.85	0.00156	0.3057	0.0175
10.06	4.80	0.00405	0.7933	0.0282
15.02	8.90	0.00750	1.4708	0.0384
20.33	14.50	0.01223	2.3963	0.0490
25.09	21.00	0.01771	3.4705	0.0589
29.45	27.70	0.02336	4.5777	0.0677
35.18	36.20	0.03052	5.9825	0.0773
40.26	45.70	0.03853	7.5524	0.0869
45.12	55.50	0.04680	9.1720	0.0958
50.13	63.20	0.05329	10.4445	0.1022

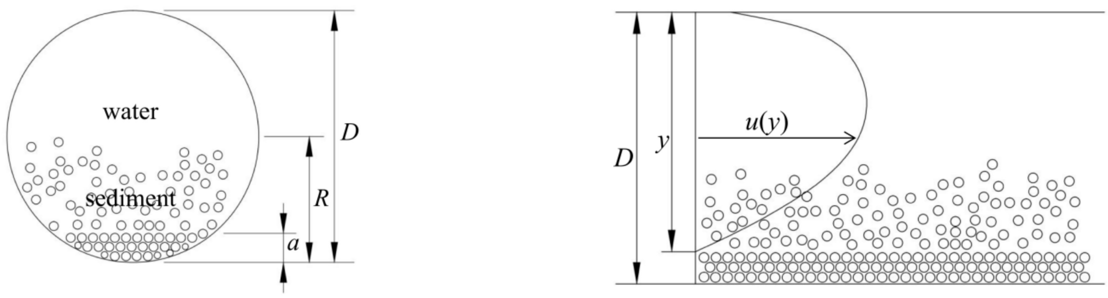

(**a**) (**b**)

Figure 6. Schematic diagram of water–sediment two-phase flow in the pipe: (**a**) section; and (**b**) longitudinal.

Compared with those of clear water, the physical and movement characteristics of sediment-laden flow changed significantly. The increase in sediment concentration resulted in an increase in the bulk density of muddy water, which led to the corresponding change in settlement regularity and the rheological characteristics of sediment-laden flow [31]. The velocity characteristics of water–sediment two-phase flow are much more complex than those of clear water flow. The interaction between the sediment particles and surrounding water changes the rheological characteristics of the flow, and the velocity structure changes significantly. Figure 7 shows the vertical distribution of velocity in the pipe caused by the change in sediment concentration under different flow rate conditions. The most obvious change is from the axisymmetric velocity distribution of clear water to the nonaxisymmetric distribution.

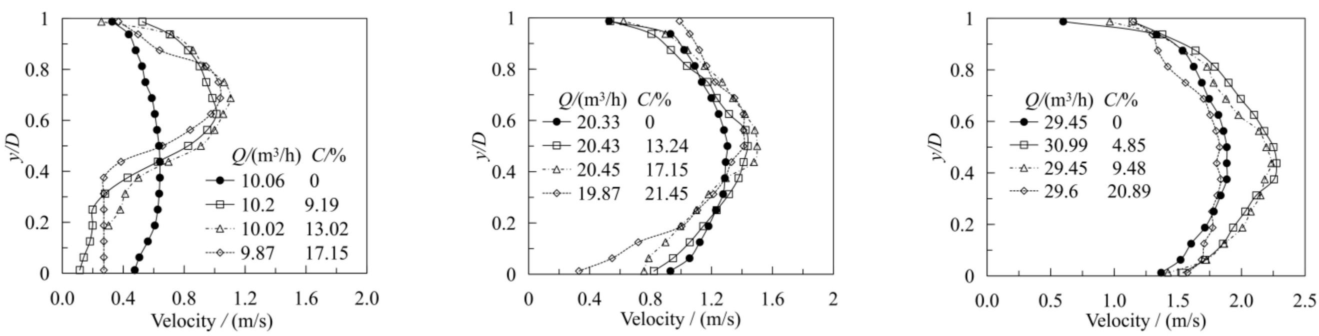

(**a**) (**b**) (**c**)

Figure 7. Vertical distribution of observed velocity for different flow rates: (**a**) Q = 9.87–10.2 m^3/h; (**b**) Q = 19.87–20.45 m^3/h; and (**c**) Q = 29.45–30.99 m^3/h.

When the flow rate is approximately 10 m^3/h (Figure 7a), sliding beds or sediment deposition occurs at the bottom of the pipe with increasing sediment content, and the vertical velocity distribution has an obvious change compared with that of clear water. The maximum velocity is greater than that of clear water and located in the region above the pipe center (y/D = 0.5). The sediment concentration affects the flow turbulence; especially when there is a sliding bed or deposition at the bottom of the pipe, the suspended sediment concentration in this region is relatively high, and the velocity gradient significantly increases. When the sediment concentration increased to 9.19%, the maximum velocity increased to 0.6 (y/D), and the velocity distribution changed little in the range of 0–0.3. However, the velocity gradient in the region from 0.3 to 0.6 was significantly larger than that in other regions. When the sediment concentration increased to 17.15%, the maximum velocity increased to 0.7 (y/D), and the thickness of the sediment sliding bed at the bottom of the pipe further increased. The velocity distribution in the region below 0.4 was basically the same, showing signs of laminar flow movement.

When the flow rate increased to approximately 20 m^3/h (Figure 7b), the velocity structure changed significantly. When the sediment concentration gradually increased from 13.24 to 21.45%, the velocity gradient in the region below 0.5 gradually increased and the maximum velocity increased and was greater than the maximum velocity of clear water, which led to asymmetry in the section velocity distribution. When the flow rate was approximately 30 m^3/h (Figure 7c), the hydrodynamic condition was enhanced, the sediment-carrying capacity was further improved and the asymmetry of the velocity distribution was significantly reduced.

3.2. Sediment Concentration Distribution

In the turbulent sediment transport process in circular pipes, continuous exchanges occurred between the upper and lower water layers due to water flow turbulence. The concentration profiles along the vertical direction show that the low concentration near the top and high concentration near the bed are affected by the gravity effect of sediment particles. In this paper, several types of vertical distributions of sediment concentration in pipes under constant uniform flow are summarized, as shown in Figure 8.

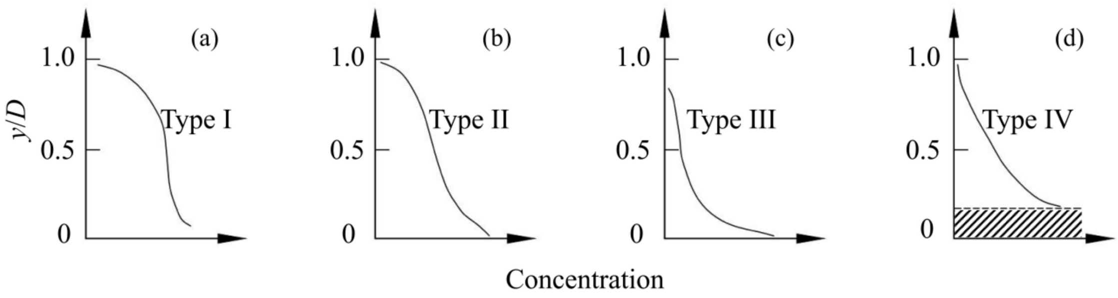

Figure 8. Concentration profiles: (**a**) Type I, homogeneous flow; (**b**) Type II, heterogeneous flow; (**c**) Type III, heterogeneous flow with a sliding bed; and (**d**) Type IV, heterogeneous flow with a sedimentary layer.

For stable and uniform pipe flow, the sediment concentration C varies with distance y from the pipe wall. Under the condition of low flow, the sediment-carrying capacity is weak, and the concentration of sediment particles becomes increasingly large near the bed as the sediment concentration increases. For the area near the top of the pipe, the velocity is smaller than that in the central region due to the resistance of the pipe wall. Additionally, the sediment concentration is obviously smaller because of the self-gravity effect of the sediment particles [32], and the vertical concentration distribution tends to be low in the upper layer and high in the lower layer. Under conditions of large flow, the hydrodynamic conditions are enhanced, and the sediment particles of the bottom pipe are disturbed and suspended when the turbulent velocity fluctuations are sufficiently large to maintain the particles [33]. Figure 9 shows the distribution of sediment concentrations along the vertical direction in the test section of the pipe.

When the flow rate is approximately 10 m^3/h, the vertical concentration profile shows the distribution characteristics of a low concentration in the upper region and a high concentration in the lower region, corresponding to the Type IV profile. With an increase in the flow rate to a value such as approximately 20 m^3/h, the vertical concentration distribution of high sediment-laden flow in the pipe is significantly different from that of low sediment-laden flow, and the concentration profile changes from Type III to Type II when the sediment content gradually increases. When the flow rate is further increased to approximately 30 m^3/h, the hydrodynamics are further enhanced, and the vertical concentration profile gradually tends to become uniformly distributed from top to bottom (Type I). It is clearly seen that at a given flow rate with an increase in sediment concentration, the concentration at the bottom and top of the pipe approaches unity, which implies that the sediment concentration decreases in the lower half and increases in the upper half [34].

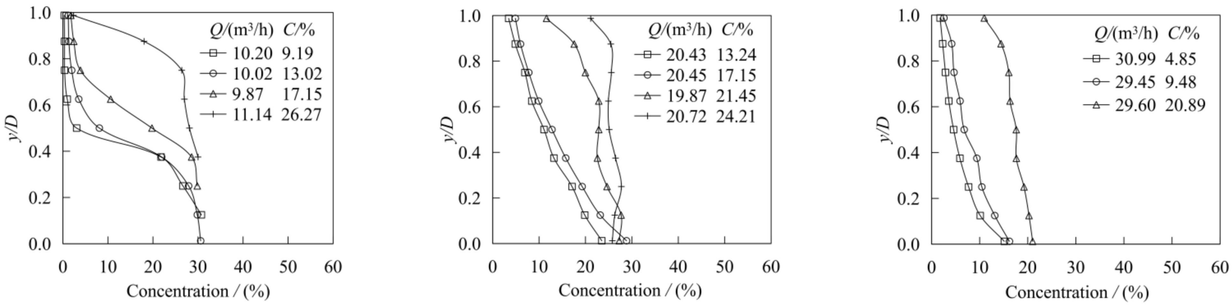

(**a**) (**b**) (**c**)

Figure 9. Vertical distribution of measured sediment concentrations in pipes for different discharges: (**a**) Q = 9.87–11.14 m^3/h; (**b**) Q = 19.87–20.72 m^3/h; and (**c**) Q = 29.45–30.99 m^3/h.

3.3. Influence of Sediment Concentration on the Resistance Coefficient

The pipeline resistance coefficient f is generally described by the Darcy–Weisbach Equation (2). In the sediment transport process in pipes, the resistance is affected by the rheological characteristics of hyperconcentrations, which are very different from clear water. Resistance loss for pipe sediment-laden flows directly affects the sediment transport capacity. The flow velocity, sediment concentration, sediment particle composition and other factors will affect the resistance coefficient. Here, we mainly analyzed the influence of sediment concentration on the resistance coefficient.

The pipe head loss due to friction is obtained from the Darcy–Weisbach equation:

$$h_f = f \frac{L}{D} \frac{V^2}{2g} \tag{2}$$

where f is the resistance coefficient; L is the length of the pipe over which the loss occurs; h_f is the head loss due to viscous effects; g is the gravitational acceleration; D is the pipe diameter; and V is the mean velocity of the pipe section.

As shown in Figure 10, at the same flow rate, the resistance coefficient f increases with the sediment concentration in the pipe. In addition, as the sediment concentration increased, the resistance coefficient at a flow rate of 20 m^3/h was significantly faster than that at a flow rate of 30 m^3/h. Under the same transportation conditions, the sediment concentration increase means that the solid volume fraction in the unit volume increases and the collision of the interparticle increases. This also increases the energy of water used to support the particle suspension and increases the pipeline resistance loss [35].

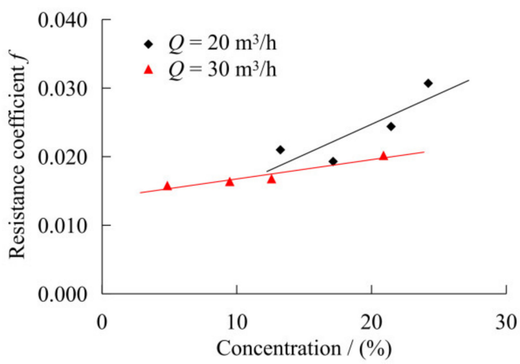

Figure 10. The influence of sediment concentration on the resistance coefficient.

3.4. Sediment Transport Flux and Sediment Sorting

3.4.1. Sediment Transport Flux

The sediment concentration and velocity determine the sediment transport capacity of the pipe. Under the given flow conditions, many sediment transport equations can predict the sediment transport capacity of a given sediment. Existing sediment transport formulas can be classified into several categories due to their basic approaches [33]: (1) sediment transport formulas based on convection; (2) sediment transport formulas based on the energy dissipation rate; and (3) graphic methods and empirical formulas based on regression analysis. The cross-sectional velocity and sediment concentration distribution of the pipe under stable and uniform conditions were obtained through the experiment, and the sediment flux in the vertical line was graphically calculated. A schematic diagram of the velocity and sediment concentration in the pipe is shown in Figure 11.

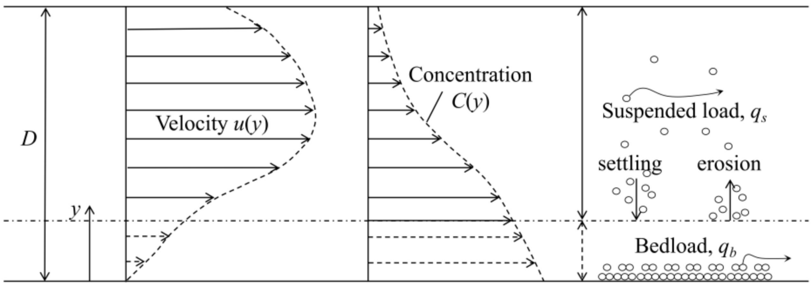

Figure 11. Sketch of the velocity distribution, concentration profile, as well as the sediment settling and erosion processes (modified from Julien, 2010 [33]).

The total sediment transport discharge per unit width q can be calculated from the sum of the unit bed sediment transport discharge q_b and the unit suspended sediment transport discharge q_s from Equation (3):

$$q = q_b + q_s = q_b + \int_a^D C u_x dz \tag{3}$$

where q is the total sediment transport discharge per unit width; q_b is the bed load transport discharge per unit width; q_s is the suspended load transport discharge per unit width; u_x is the time-averaged velocity; a is the reference elevation above the pipe wall; z is the elevation above the reference elevation; and D is the pipe diameter.

For a certain section of the pipe, the sediment flux at different heights y can be expressed as the product of the average velocity $\overline{u_i}$ and sediment concentration $\overline{c_i}$, i.e., $q_i = \overline{u_i c_i}$. According to the physical process of sediment transport, the sediment transport flux at different heights in a certain section of the pipe can be calculated by using Equation (2). This research aimed to obtain the vertical distribution of sediment transport discharge per unit width of the center section, and the results are shown in Figure 12.

At a low flow rate of 10 m^3/h (Figure 12a), there are different degrees of sediment deposits or sliding layers in the pipe bottom with increasing sediment content. The vertical velocity gradually tends toward zero near the bed, resulting in the sediment flux approaching zero in this region, while the maximum sediment flux zone gradually moves up with increasing bottom sedimentary layer thickness. When the flow rate reaches 20 m^3/h (Figure 12b), the maximum sediment transport flux zone in the pipe gradually moves up with increasing sediment content, the maximum sediment transport intensity is generally located in the pipe center (y/D = 0.5), and the maximum velocity is also located in this region. With the increase in sediment content in the pipe, the sediment transport characteristics change, unlike those under the low-concentration flow condition. When the flow rate increases to 30 m^3/h (Figure 12c), the profile of the velocity and sediment concentration tends to distribute evenly along the vertical direction with increasing sediment content, and the overall sediment transport intensity increases. Under high-concentration flow conditions, the settling velocity of sediment particles decreases, and the gravity effect is relatively weakened. Additionally, the number of collisions between particles increases and the sediment concentration distribution is relatively uniform, which leads to the strong sediment-carrying capacity of the hyperconcentrated flow.

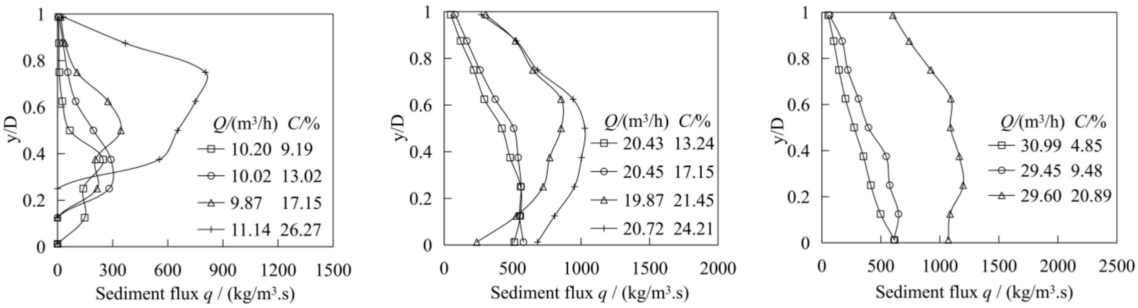

(**a**) (**b**) (**c**)

Figure 12. Distribution of sediment transport flux per unit width: (**a**) Q = 9.87–11.14 m^3/h; (**b**) Q = 19.87–20.72 m^3/h; and (**c**) Q = 29.45–30.99 m^3/h.

3.4.2. Sediment Sorting

Under natural conditions, the movement and deposition of solid–liquid two-phase flow are often accompanied by the separation of solid particles. The temporal and spatial separation information of these particles is of great significance for the analysis of environmental climate change, geomorphic evolution and the movement mechanism of solid–liquid two-phase flow [13]. Sediment sorting is a process of adjustment caused by the energy conversion and continuous dissipation of sediment-laden flow. The interactions between flow turbulence and sediment settlement affect each other. The gradient of the sediment concentration distribution along the vertical direction and the turbulence intensity of the water flow are the main factors affecting sediment settling and sorting [36]. In this experiment, sediment samples with different sediment concentrations were obtained by the stratified sampling method, and an ultrafast Malvern 3000 intelligent particle size analyzer was used to analyze the particle sizes in each group of sediment samples.

Figure 13 shows sediment sorting caused by sediment concentration under different flow conditions. (1) When Q = 10.2 m^3/h and C = 9.19%, the sediment gradation at different positions along the vertical direction obviously changes. The slope of the sediment gradation curve decreased from bottom to top (Figure 13a) and the sediment particle size distribution became progressively uniform. The sediment composition in the range below the pipe center (y/D = 0.5) was very uneven and was mainly dominated by coarse particles. For sediment particles with y/D values above 0.5, the proportion of fine sediment obviously increased, and the size composition of the upper sediment was more uniform and mainly dominated by fine particles. (2) When Q = 10.02 m^3/h, C = 13.02% and Q = 9.87 m^3/h, and when C = 17.15%, the sediment deposition thickness in the pipe bottom increases, the composition of the sediment particles below 0.5 is still uneven, and the proportion of coarse particles in the sediment is still large. Sediment with values above 0.5 presents different layers, the grading curve is obvious and the volume density of the fine sediment gradually increases.

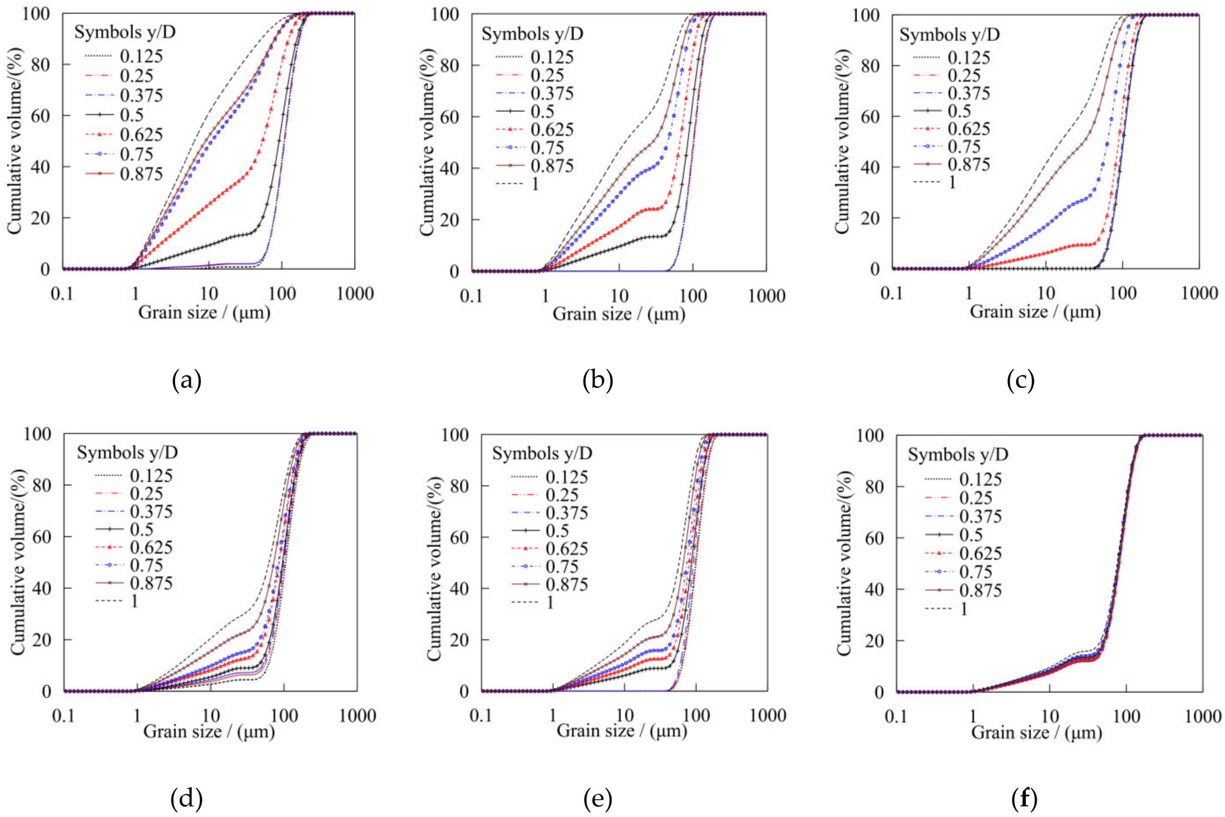

Figure 13. Sediment sorting with different sediment concentrations: (**a**) Q = 10.2 m^3/h; C = 9.19%; (**b**) Q = 10.02 m^3/h; C = 13.02%; (**c**) Q = 9.87 m^3/h; C = 17.15%; (**d**) Q = 20.43 m^3/h; C = 13.24%; (**e**) Q = 20.45 m^3/h; C = 17.15%; and (**f**) Q = 20.72 m^3/h; C = 24.21%.

When Q = 20.43 m^3/h and C = 13.24%, obvious stratification of the sediment grading curve still occurred along the vertical direction, and the proportion of fine particles in the sediment gradually increased from bottom to top in the pipe; however, the coarse particles still accounted for a large proportion of the sediment (Figure 13d). When Q = 20.72 m^3/h and C = 24.21%, the composition of the sediment particles along the vertical direction was basically the same, and the gradation curve had no significant change (Figure 13f). In addition, the effect of sediment sorting progressively weakened, and coarse particles in the sediment were still the main component. The interaction forces between solid particles included Coulomb friction, collision stress and dispersion stress. When the concentration of particles is high, collisions between particles are dominant [13]. At the same flow rate, the increase in sediment concentration leads to the enhancement of collisions between particles, and the ascending effect of coarse particles is obviously strengthened [37]. The free movement distance between suspended sediment particles is reduced, and the number of collisions increases, weakening the separation of coarse and fine particles.

In sediment-laden flow, there is always relative movement between the sediment particles and the surrounding water. The increase in sediment particles restricts the turbulent development of the flow; however, the number of particle–particle collisions increases, the sedimentation of coarse particles is limited to a certain extent, and the separation strength of sediment particles is also relatively reduced.

To further illustrate the vertical separation effect of sediment particles, a specific analysis of the median particle size (d_{50}) of sediments at different heights was carried out. Figure 14 shows the distribution of the median particle size (d_{50}) along the vertical direction at different discharges and sediment concentrations. Under low-discharge conditions, the median grain size of the sediment particles varied greatly along the vertical direction gradually, with a gradual decrease from 100–116 μm at the pipe bottom to 5–20 μm at the pipe top (Figure 14a). When the flow rate was approximately 20 m^3/h, the vertical change in the median particle size was weakened, and the vertical change in the median particle size was small with increasing sediment content. For example, when the sediment concentration was 24.21%, the median sediment particle size hardly changed along the vertical direction, as shown in Figure 14b. When Q = 30 m^3/h and C = 20.89%, the median sediment particle size was uniformly distributed along the vertical direction, and there was no obvious change (Figure 14c). At high transportation velocities, the sediment particles are generally uniformly distributed across the cross-section of the pipe [38]. The reason for this is that the average free moving distance between sediment particles is reduced, and the dense particle arrangement inhibits the generation and development of larger-scale turbulent eddies, weakening the separation effect of coarse and fine particles in the vertical direction [39,40].

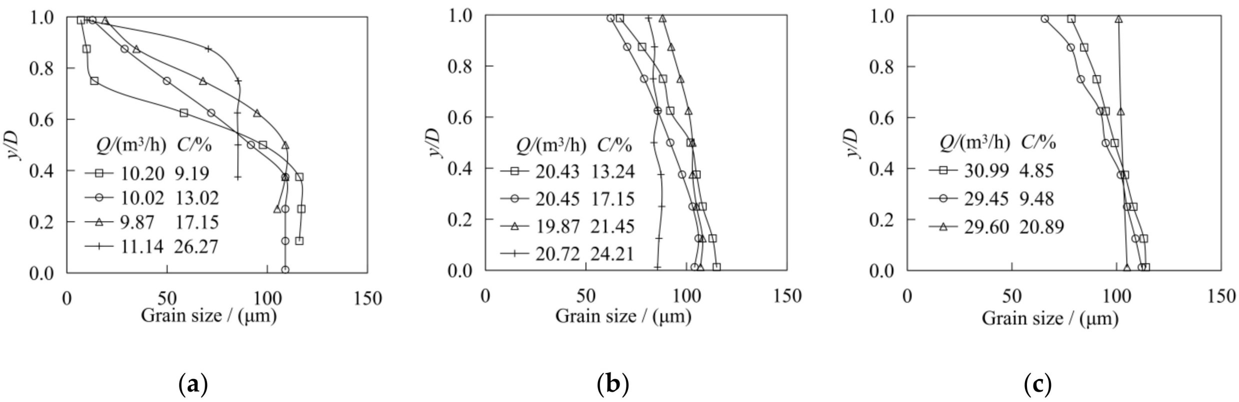

Figure 14. Distribution of the median particle size (d_{50}) along the vertical direction at different sediment concentrations and different discharges: (**a**) Q = 9.87–11.14 m^3/h; (**b**) Q = 19.87–20.72 m^3/h; and (**c**) Q = 29.45–30.99 m^3/h.

Pipeline transport is widely used in river sediment engineering applications, such as flood discharge and sediment discharge in upstream reservoirs, diversion and sediment diversion along the river channel, dredging in downstream river channels and siltation in floodplains, due to its efficient sediment transfer capacity. The optimal allocation of water and sediment resources in the river plays an active role in promoting the recovery of reservoir capacity, maintaining the stability of the river channel and improving the soil fertility of floodplain areas. The sediment-carrying flow structural change and the sediment sorting mechanism were experimentally determined at different sediment concentrations; these results can provide technical support for flood discharging and sediment flushing, reservoir capacity restoration and channel dredging.

3.5. Limitations and Uncertainties

The movement of water–sediment in pipelines is actually a complicated movement of solid–liquid two-phase flow, which is much more complicated than that in open channels. In this experiment, there were the following limitations and uncertainties.

The measurement accuracy of the local velocity in the pipe depends on the distance between the total and static tubes, the rheological behavior of the fluid and the Reynolds number. When the Reynolds number is low, frictional losses become predominant over the dynamic pressure term, and the measured pressure difference is not an adequate representation of the kinetic energy transformation. Additionally, the rheological behavior of the fluid plays a key role in the accuracy of the measurements [41]. In addition, the sediment concentrations at different heights are obtained by using a Pitot tube. When the sediment in the pipeline is too large, it easily causes internal blockage. When this happens, it is necessary to flush the blocked sediment via water injection and then perform a retest to obtain the sediment concentration.

There are many factors that will affect pipeline sediment transportation, such as diameter, pipeline material characteristics and sediment particle sizes. The relevant data in this study were obtained from tests performed in a pipe with an inner diameter of 80 mm. For slurry pipeline transportation, the boundary effect of an 80 mm inner diameter is relatively obvious compared to that of pipes with large diameters of hundreds of millimeters or more in the project. Therefore, the experimental results could only perform qualitative analysis. Regarding the transformation of experimental results to practical engineering, we need to consider the Reynolds similarity and resistance similarity, which will be further explored in subsequent experiments.

4. Conclusions

Through the design of a horizontal pressured sediment transport pipeline test model, nonuniform sediment (d_{50} = 107 μm) was used as the experimental material, and the distributions of the velocity and sediment concentration for a variety of hyperconcentrated and dilute flows were studied. The detailed conclusions are as follows.

Under conditions of low flow rate (Q = 10 m^3/h), the thickness of the sliding bed or sedimentary layer at the bottom of the pipe increases with increasing sediment content. The maximum velocity zone moves up significantly, and the asymmetry of the velocity profile becomes large. The low-velocity hydrodynamic force is weak, and the vertical sediment particles are obviously stratified. The pipe bottom area is dominated by coarse-grained sediment (d_{50} = 110–125 μm), and the fine-grained sediment ($d_{50} \leq 90$ μm) is mostly concentrated in the upper area. At the same flow rate, the sediment flux in the central area of the pipe increases with increasing sediment content.

When sediment transport is driven by a large flow rate ($Q \geq 20$ m^3/h), there is little or no sediment at the bottom of the pipe, and most of the sediment moves forward in the form of a suspended load. The sediment-carrying capacity of the water flow increases, and the asymmetry of the velocity profile distribution is reduced. With the increase in the sediment content, the concentration profile gradually transforms from the "upper small, lower large" type to a uniform type, and the sediment transport capacity in the pipe increases accordingly. When Q = 20.72 m^3/h and C = 24.21% and when Q = 29.60 m^3/h and C = 20.89%, the sediment concentration profile becomes uniformly distributed along the vertical direction, the separation effect of sediment particles weakens, and the median particle size (d_{50}) does not change much along the vertical line.

This paper mainly discussed the technical engineering issues of sediment transport and sorting in horizontal pipelines. The characteristics of the flow velocity structure, concentration profile, sediment transport flux and sediment sorting that vary with flow rate and sediment content were studied, and the interaction mechanism between sediment and water flow was revealed. These research results can provide some references for reservoir flooding and sediment discharging, river dredging and floodplain area deposition.

Author Contributions: Conceptualization, Y.L. and J.Z.; Data curation, H.X.; Methodology, Y.L. and Y.B.; Project administration, J.Z. and Y.B.; Supervision, J.Z. and Y.B.; Validation, H.X.; Writing—Original draft, Y.L.; Writing—Review and Editing, Y.L. and H.X. All authors have read and agreed to the published version of the manuscript.

Funding: This research was funded by the National Natural Science Foundation of China, grant numbers 51979185 and 51879182 and the National Key R&D Programme of China, grant number 2016YFC0402503.

Institutional Review Board Statement: Not applicable.

Informed Consent Statement: Not applicable.

Data Availability Statement: Data is contained within the article.

Acknowledgments: The authors are grateful to Wenli Hu for his help with the experiments in this paper. In addition, we would like to thank the reviewers very much for their valuable comments and suggestions.

Conflicts of Interest: The authors declare no conflicts of interest.

References

1. Chebbo, G.; Bachoc, A. Characterization of Suspended Solids in Urban Wet Weather Discharges. *Water Sci. Technol.* **1992**, *25*, 171–179. [CrossRef]
2. Mcilhatton, T.D.; Ashley, R.M.; Tait, S.J. Improved formulations for rapid erosion of diverse solids in combined sewers. *Water Sci. Technol.* **2005**, *52*, 143–150. [CrossRef]
3. Schmitt, T.G.; Thomas, M.; Ettrich, N. Assessment of urban flooding by dual drainage simulation model RisUrSim. *Water Sci. Technol.* **2005**, *52*, 257–264. [CrossRef] [PubMed]
4. Danielson, T.J. Sand transport modeling in multiphase pipelines. In Proceedings of the Offshore Technology Conference, Houston, TX, USA, 30 April–3 May 2007.
5. Hashemi, S.A.; Sadighian, A.; Shah, S.; Sanders, R.S. Solid velocity and concentration fluctuations in highly concentrated liquid–solid (slurry) pipe flows. *Int. J. Multiph. Flow* **2014**, *66*, 46–61. [CrossRef]
6. Najmi, K.; Hill, A.L.; Mclaury, B.S.; Shirazi, S.A.; Cremaschi, S. Experimental study of low concentration sand transport in multiphase air-water horizontal pipelines. *J. Energy Resour. Technol.* **2015**, *137*, 32908. [CrossRef]
7. Dabirian, R.; Mohan, R.; Shoham, O.; Kouba, G. Critical sand deposition velocity for gas-liquid stratified flow in horizontal pipes. *J. Nat. Gas Sci. Eng.* **2016**, *33*, 527–537. [CrossRef]
8. Bai, Y.C.; Xu, H.J. Hydrodynamic instability of hyperconcentrated flows of the Yellow River. *J. Hydraul. Res.* **2010**, *48*, 742–753. [CrossRef]
9. Xu, H.J.; Bai, Y.C.; Li, C. Hydro-instabilitycharacteristics of Bingham fluidflow as in the Yellow River. *J. Hydro-Environ. Res.* **2018**, *20*, 22–30. [CrossRef]
10. Bagnold, R.A. Some flume experiments on large grains but little denser than the transporting fluid, and their implications. *Proc. Inst. Civ. Eng.* **1955**, *4*, 174–205. [CrossRef]
11. Wang, Z.Y.; Zeng, Q.H.; Zhang, X.Y. Experimental study of solid-nonnewtonian fluid two-phase flow. *J. Sediment Res.* **1990**, *3*, 1–12. (In Chinese)
12. Liu, Q.Q.; Chen, L. Further analysis of the effect of particles on flow turbulence. *J. Hydraul. Eng.* **1997**, 77–82. (In Chinese)
13. Ni, J.R.; Qu, Y.Z. Modeling of vertical segregation of solid particles in sediment-laden flow. *J. Hydrodyn.* **2003**, *18*, 349–353. (In Chinese)
14. Qiang, T.; Collins, A.L.; Wen, A.; He, X.; Bao, Y.; Yan, D.; Yi, L.; Zhang, Y. Particle size differentiation explains flow regulation controls on sediment sorting in the water-level fluctuation zone of the Three Gorges Reservoir, China. *Sci. Total Environ.* **2018**, *633*, 1114.
15. Shi, Z.H.; Fang, N.F.; Wu, F.Z.; Wang, L.; Yue, B.J.; Wu, G.L. oil erosion processes and sediment sorting associated with transport mechanisms on steep slope. *J. Hydrol.* **2012**, *454–455*, 123–130. [CrossRef]
16. Nag, D.; Phartiyal, B.; Singh, D.S.; Ariztegui, D.J.S. Sedimentary characteristics of palaeolake deposits along the Indus River valley, Ladakh, Trans-Himalaya: Implications for the depositional environment. *Sedimentology* **2016**, *63*, 1765–1785. [CrossRef]
17. Han, Q.W.; Yang, X.Q. A review of the research work of reservoir sedimentation in China. *J. China Inst. Water* **2003**, *1*, 169–178. (In Chinese)
18. Caviedes-Voullième, D.; Morales-Hernández, M.; Juez, C.; Lacasta, A.; García-Navarro, P. Two-Dimensional Numerical Simulation of Bed-Load Transport of a Finite-Depth Sediment Layer: Applications to Channel Flushing. *J. Hydraul. Eng.* **2017**, *143*, 4017034. [CrossRef]
19. Jha, S.K.; Bombardelli, F.A. Two-phase modeling of turbulence in dilute sediment-laden, open-channel flows. *Environ. Fluid Mech.* **2009**, *9*, 237–266. [CrossRef]
20. Pu, J.H.; Wallwork, J.T.; Khan, M.A.; Pandey, M.; Gough, T. Flood Suspended Sediment Transport: Combined Modeling from Dilute to Hyper-Concentrated Flow. *Water* **2021**, *13*, 379. [CrossRef]
21. Liang, L.; Yu, X.; Bombardelli, F. A General Mixture Model for Sediment Laden Flows. *Adv. Water Resour.* **2017**, *107*, 108–125. [CrossRef]
22. Wang, J.; Li, Y.; Pan, L.; Lai, Z.; Jian, S. Study of the Sediment Transport Law in a Reverse-Slope Section of a Pressurized Pipeline. *Water* **2020**, *12*, 3042. [CrossRef]
23. Al-Lababidi, S.; Yan, W.; Yeung, H. Sand Transportations and Deposition Characteristics in Multiphase Flows in Pipelines. *J. Energy Resour. Technol.* **2012**, *134*, 34501. [CrossRef]
24. Manuel, R.P.; Jose, A.; Joaquín, S.; Jerónimo, P.; Alfredo, J.; Juan, N. Characterization of sediments during transport of solids in circular sewer pipes. *Water Sci. Technol.* **2018**, *2017*, wst2018055. [CrossRef]
25. Montes, C.; Kapelan, Z.; Saldarriaga, J. Predicting nondeposition sediment transport in sewer pipes using Random forest. *Water Res.* **2020**, *189*, 116639. [CrossRef]
26. Wu, J.D.; Yuan, X.Y.; Fan, Y.G.; Wang, X.D. State Modeling and Verification of Resistance Loss along the Long-Range Solid-Liquid Two-Phase Pipeline. *Adv. Mater. Res.* **2012**, *461*, 854–859. [CrossRef]
27. Shuai, M.; Wang, X.; Wu, J.; Leng, T.; Jiang, D. Study on resistance loss characteristics of iron concentrate pipeline transportation. In Proceedings of the The 27th Chinese Control and Decision Conference (2015 CCDC), Qingdao, China, 23–25 May 2015; pp. 2037–2041. [CrossRef]

28. Wang, Z.; Qian, N. Experiment study of two–Phase turbulent flow with hyperconcentration of coarse particles. *Sci. China Ser. A* **1984**, *XXVII*, 1317–1327.
29. Xie, C.G.; Atkinson, I.; Hammond, P.; Oddie, G.; Bolchover, P. Isokinetic Sampling: US. US7717000 B2, 18 May 2010.
30. Cheng, P.; Gao, S.; Li, X.L. Evaluation of a Wide Range Laser Particle Size Analyses and Comparison with Pipette and Sieving Methods. *Acta Sedimentol. Sin.* **2001**, *19*, 449–455. (In Chinese)
31. Wang, Z.Y.; Chien, N. Experimental study on the movement law of laminated load. *Sci. China Ser. A* **1984**, *1*, 91–98. (In Chinese)
32. Archibong-Eso, A.; Aliyu, A.M.; Yan, W.; Okeke, N.E.; Baba, Y.D.; Fajemidupe, O.; Yeung, H. Experimental Study on Sand Transport Characteristics in Horizontal and Inclined Two-Phase Solid-Liquid Pipe Flow. *J. Pipeline Syst. Eng. Pract.* **2020**, *11*, 4019050. [CrossRef]
33. Julien, P.Y. *Erosion and Sedimentation*; Cambridge University Press: New York, NY, USA, 2010.
34. Kaushal, D.R.; Tomita, Y. Comparative study of pressure drop in multisized particulate slurry flow through pipe and rectangular duct. *Int. J. Multiph. Flow* **2003**, *29*, 1473–1487. [CrossRef]
35. Verma, A.K.; Singh, S.N.; Seshadri, V. Pressure drop for the flow of high concentration solid-liquid mixture across 90° horizontal conventional circular pipe bend. *Indian J. Eng. Mater. Sci.* **2006**, *13*, 477–483.
36. Peng, R.S.; Li, H.M.; Liu, Y.Z.; Yang, W.H. Dynamic settling velocity of sediment and improvement of quasi-hydrostatic settlement method. *J. Sediment Res.* **1997**, *2*, 74–78. (In Chinese)
37. Qu, Y.Z.; Ni, J.R.; Meng, X.G. Mechanism of vertical segregation of solid particles in sediment-laden flow. *J. Hydrodyn.* **2003**, *18*, 108–113.
38. Kaushal, D.R.; Tomita, Y.; Dighade, R.R. Concentration at the pipe bottom at deposition velocity for transportation of commercial slurries through pipeline. *Powder Technol.* **2002**, *125*, 89–101. [CrossRef]
39. Wang, Z.; Qian, N. Experimental study on the physical properties of sediment suspensions with hyperconcentration. *J. Hydraul. Eng.* **1984**, *4*, 3–12. (In Chinese)
40. Spearman, J.; Manning, A.J. On the hindered settling of sand-mud suspensions. *Ocean Dyn.* **2017**, *67*, 465–483. [CrossRef]
41. Etemad, S.G.; Thibault, J.; Hashemabadi, S.H. Calculation of the Pitot tube correction factor for Newtonian and non-Newtonian fluids. *ISA Trans.* **2003**, *42*, 505–512. [CrossRef]